2019 Rock Dynamics Summit– Aydan et al. (eds)
© 2019 Taylor & Francis Group, London, ISBN 978-0-367-34783-3

An experimental study on the effects of earthquake faulting on rock engineering structures

Y. Ohta
Graduate School of Science and Technology, Tokai University, Shizuoka, Japan (Presently with Nuclear Energy Regulation Authority), Shizuoka, Japan

Ö. Aydan
Department of Civil Enineering, University of the Ryukyus, Okinawa, Japan

ABSTRACT: The authors performed some laboratory model experiments on faulting and various rock engineering structures subjected to thrust, normal and strike-slip faulting movements under dynamic condition. Several experiments were carried out to investigate the effect of faulting on the slopes, underground openings, bridges and its foundations, and embedded linear structures. Model experiments were carried out using breakable blocks and layers. The experiments showed that the faulting mode and discontinuity orientation have great affect on the failure mode of various structures.

1 INTRODUCTION

Ground motion characteristics, deformation and surface breaks of earthquakes depend upon the causative faults. Their effects on the seismic design of engineering structures are almost not considered in the present codes of design although there are attempts to include in some countries (i.e. USA, Japan, Taiwan, Turkey (Aydan et al. 1999, 2009a,b,c).

The experimental device is developed amd used for investigating the effect of faulting under gravitational field. The orientation of faulting can be adjusted as desired (Ohta 2011; Ohta & Aydan 2010). The maximum displacement of faulting of the moving side of the faulting experiments was varied between 25 and 100mm. The base of the experimental set-up can model rigid body motions of base rock and it has a box of 780 mm long, 250 mm wide and 300 mm deep. This experimental device is used to investigate the effect of forced displacement due to faulting on rock slopes and underground openings. The displacement and accelerations were measured simultaneously.

Several experiments were carried out to investigate the effect of faulting on bridge and its foundations. Model experiments were carried out using either breakable blocks and layers or non-breakable blocks. The authors have been also performing some model experiments on the effect of faulting on the stability and failure modes of shallow undergound openings. In this study, the authors carried out some laboratory experiments to simulate the motions during normal and thrust faulting and their effects on model structures to investigate the effects of faulting due to earthquakes. They summarize the findings from this experimental study and their implications in practice.

2 MODEL EXPERIMENTS

2.1 *Experimental Device*

An experimental device shown in Figs. 1 and 2 was developed for model tests on faulting under dynamic condition (Ohta, 2011). One side of the device is moveable in a chosen direction to induce base movements similar to normal or thrust faulting with a different inclination. The device can simulate from 45 degrees normal faulting movement to 135 degrees thrust faulting.

The box is 780 mm long, 300 mm high and 300 mm wide. The length of the moveable side is 400 mm. The motion of the moveable side of the device

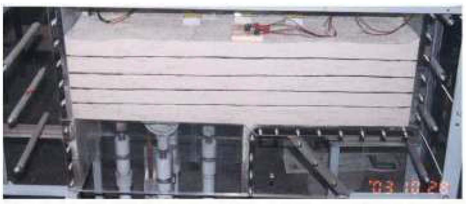

(a) A view of a faulting test with sand layer above the hard-base

(b) A view of a faulting test on a model tunnel in soft rock

Figure 1. Views of some of faulting experiments

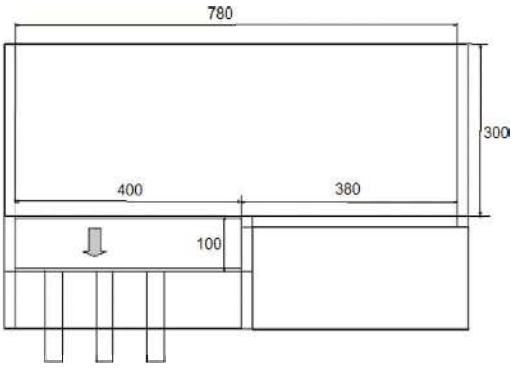

Figure 2. A drawing of the faulting test apparatus

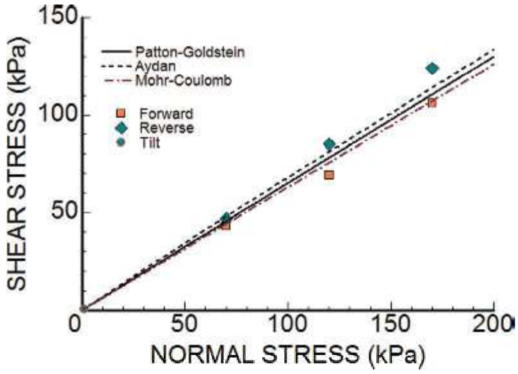

Figure 4. Shear strength envelopes of the quartz sand.

is achieved through its own weight by removing a stopper. The amount of the vertical movement of the moving base can be up to 200 mm and it can be set to a certain level as desired. The device equipped with non-contact laser displacement transducers and contact type accelerometers with three components. Besides the continuous monitoring of movements of the model ground through laser displacement transducers and accelerometers, the experiments were recorded using digital video cameras.

Layers or blocks used for physical models of layered or jointed rock mass were created through the compression of a special mixture consisting of BaSO4, ZnO and Vaseline oil under a chosen pressure. Various researchers determined the properties of this solid material. Frictional characteristics of discontinuities, unit weight, tensile and compressive strength of these samples have been measured in the laboratory as seen in Fig. 5.

2.2 *Materials*

Two kinds of ground material were considered. The first type ground model material was granular material simulating soft ground on a rigid base. The second type ground material was a rock-like material to model layered and jointed rock mass. Granular ground material on the rigid movable base is dry quartz sand. Direct shear experiments on ground material were carried out. Fig. 3 shows some of displacement vs shear stress responses. The behaviour of sand is elasto-plastic without any softening. Fig. 4 shows some yield criteria for experimental results and the friction angle of sand ranges between 32-34 degrees with an average of 33 degrees.

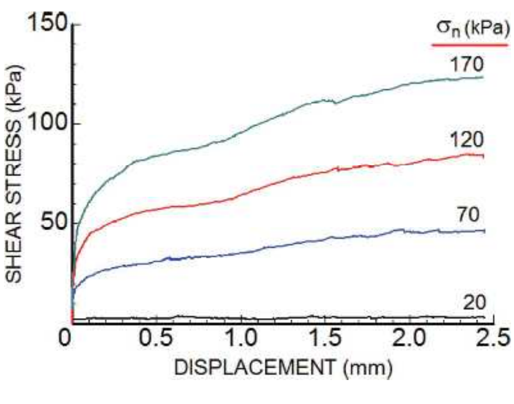

Figure 3. Shear response of sand under different normal stress.

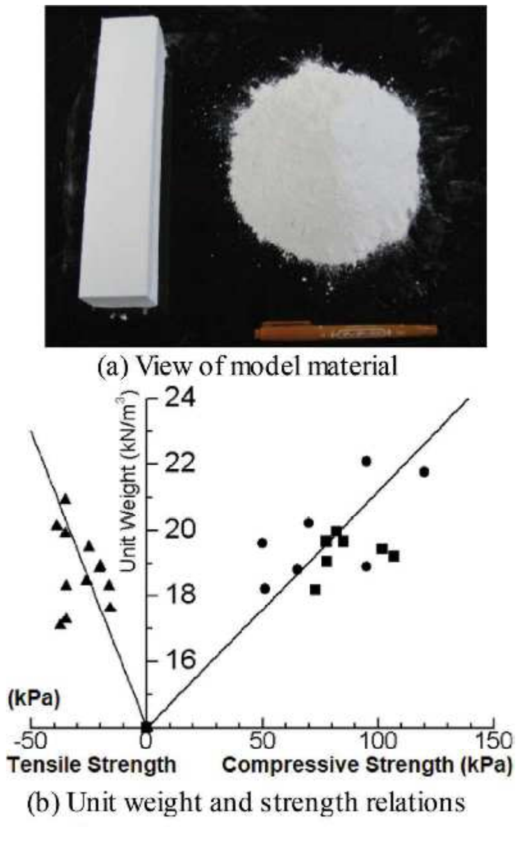

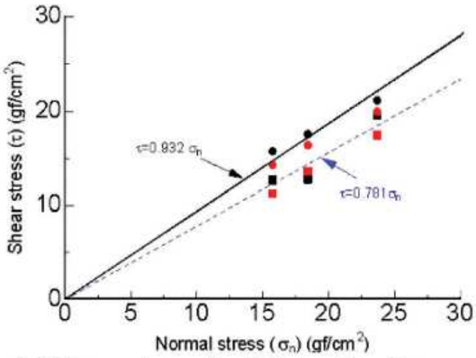

(c) Shear strength of discontinuity

Figure 5. View of rock-like model material and its mechanical properties.

3 EXPERIMENTS ON GRANULAR GROUND

The sand was poured into the soil box without any compaction. Therefore, the relative density of the sand ranges between 35-45 % with an average of 40%. Black dyed sand marker lines were set at an interval of about 50mm. However, the procedure for marker lines is extremely tedious and it is generally dificult to get perfect straight lines.

Once the soil model was prepared, the monitoring devices consisting of laser displacement transducers and accelerometers to observe ground motions on ground surface were set at three locations, specifically, movable and stationary blocks and just above the fault. Each experiment was recorded through digital video recorders and some pictures were taken during the experiment. Furthermore, variations of electric potential or electrical resistivity in relation to faulting were also measured using electrodes embedded into the soil and associated monitoring equipments for electric current and voltage in some of experiments.

The maximum displacement of faulting of the moving side of the faulting experiments was varied between 25 and 100mm. The vertical displacements of the fault was 25, 50, 75 and 100 mm. Due to the nature of the problem, the vertical component of accelerations becomes maximum among other components. Fig. 6 shows the vertical accelera-tion and displacement measured simulatenuously in the experiment with 200 mm thick soil deposit and 90 degrees normal faulting and Fig. 7 shows its motion at several time steps.

As seen from Fig. 6, the maximum acceleration of the movable side is greater than that of the stationary side. Furthermore, the maximum acceleration is observed when the movement of the movable side is restrained and the acceleration response is entirely unsymmetric while the acceleration response of the stationary side is almost symmetric. Although it is not the purpose of this manuscript to discuss and compare with observations in actual earthquakes, the responses measured during these experiments are quite similar to the observations in actual earthquakes as well as in rock fracture experiments (i.e. Ohta 2011; Ohta and Aydan, 2010). The variation of soil deposit thickness has a certain effect on the resulting accelerations. However, if the displacement of the fault is same, its effect would be small as compared with that of the variation of the fault displacement.

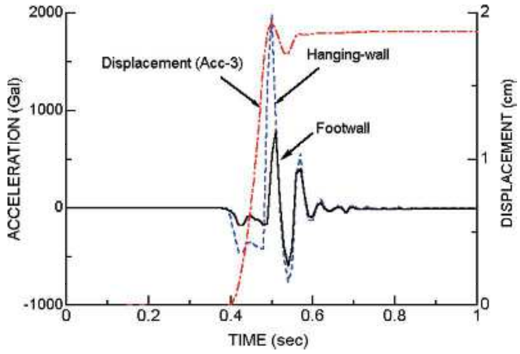

Figure 6. Acceleration responses of 200 mm thick soil deposit for 90° normal faulting.

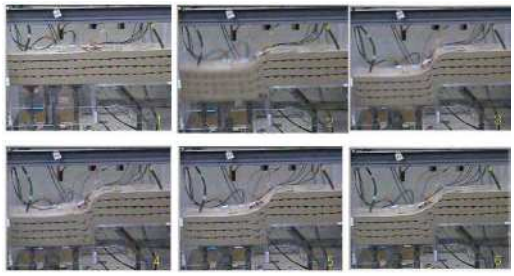

Figure 7. Motion of 200 mm thick soil deposit for 90° normal faulting.

The observations on deformation and slip-lines in experiments carried out for inclinations of 45, 90 and 135 degrees are shown in Fig. 8. Comparisons done for three different inclinations of faulting for the same amount of vertical displacements. The most extensive studies are carried out on experiments

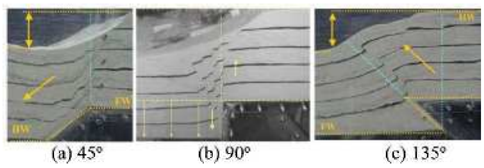

(a) 45° (b) 90° (c) 135°

Figure 8. Views of faulting experiments.

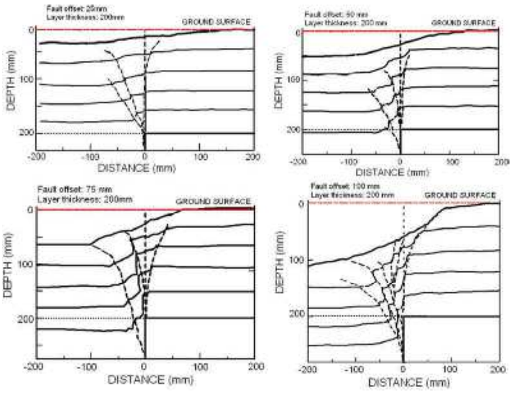

Figure 9. Sliplines in experiments with varying vertical displacement for faulting inclination of 90°.

with the faulting inclination of 90 degrees, in which the effects of allowable vertical displacements and soil thickness were investigated (Fig. 9).

The top soil deposit on the hanging wall (mobile) side is highly deformed while the soil deposit on the footwall (stationary) side is much less. Furthermore, the number slip-lines on the hanging-wall (mobile part) of the soil layer is greater than that in the footwall side. This probably associated with the amount of displacement of the mobilized soil in the hanging-wall side. It is also interesting to note that thrust type slip-lines occur at the hangingwall side while normal type slip-lines develop in the footwall side. Such slip-lines may be of great significance when ground deformation and slip-lines interpreted for faults in-situ.

The inclination of the thrust fault was set to 45 degrees and the amount of vertical displacement was varied between 40 mm and 100mm for a 200 mm soil layer. Views of soil layer after faulting are shown in Fig. 10. Similar to previous experiments, the number of slip-lines increases with the amount of fault offset. Several slip-lines develop subparallel to eact other. When the amount of fault offset is small, the slip-line does not reach ground surface and the ground surface configuration shows a flexural bend. However, if the fault offset is large enough, the top part of the soil on the hanging-wall side moves towards the footwall side and the ground deformation induces a slip-line similar to normal faults. In other words, the wedge-like body just

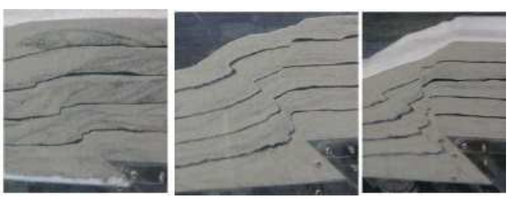

Figure 10. Views of 250 mm thick soil layer for various 45 degrees thrust fault offsets

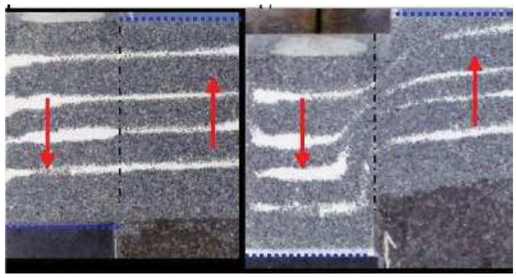

Figure 11. Negative images of several stages in a strike-slip faulting experiment in granular medium.

above the tip of the fault can not remain stable under gravitaional field and moves towards the foot-wall side and it becomes stabilized at a surface inclination equivalent to its dynamic repose angle. This is an important observation as the interpretation of ground deformation and slip-lines may be wrongly interpreted as normal faulting despite that it is a thrust faulting. Furthermore, the ground surface deformation may resemble to the ground deformation profiles resulting from classifical slope failures. This observation also implies that slope failures aligned should be interpretted as the surface expression of earthquake faulting as happened in 2005 Kashmir earthquake (Aydan et al. 2009).

In addition, some strike-slip experiments are carried out under constant velocity condition using base friction apparatus. Fig. 11 shows negative images of several stages of a strike-slip faulting experiment on a granular media. Although slip-lines were not apparent from the figure, a wide deformation band with a thickness equivalent to the amount of relative displacement developed on both sides of the projected fault-line. As noted from the figure, streching strain occur at certain direction while compressive straining occur perpendicular to the streching axis.

4 TESTS ON THE EFFECT OF FAULTING ON ENGINEERING STRUCTURES

Several model experiments were carried out to see the effect of faulting on rock engineering structures in/on rock-like ground as reported by Aydan et al. (2011). The experimental results are briefly explained in this section. Fig. 12 shows the

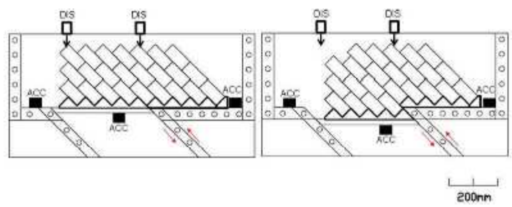

Figure 12. The instrumentation (DIS: laser displacement transducer; ACC:Accelerometer).

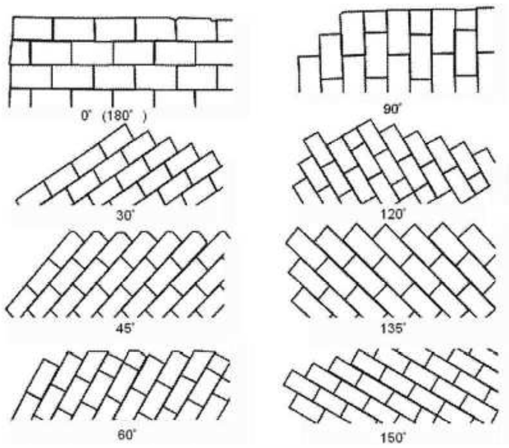

Figure 13. Illustration of experimental models of rock mass

instrumentation. Fig. 13 shows the sketches of rock mass models tested in experiments described herein.

4.1 *Underground Openings*

The authors performed some model experiments on the effect of faulting on the stability and failure modes of shallow undergound openings (Aydan et al. 2010). Fig. 14 shows views of some model experiments on shallow undergound openings subjected to the thrust faulting action with an inclination of 45°. Underground openings are assumed to be located on the projected line of the fault.

In some experiments three adjacent tunnels were excavated. While one of the tunnels was situated on the projected line of faulting, the other two tunnels were located in the footwall and hanging wall side of the fault. As seen in Fig. 14, the tunnel completely collapsed or was heavily damaged when it was located on the projected line of the faulting. When the tunnel was located on the hanging wall side, the damage was almost none in spite of the close approximity of the model tunnel to the projected fault line. However, the tunnel in the footwall side of the fault was subjected to some damage due to relative slip of layers pushed towards the slope. This simple example clearly shows the damage state may differ depending upon the location of tunnels with respect to fault movement.

4.2 *Slopes*

The authors have initiated an experimental program on the effect of faulting on the stability and failure modes of rock slopes (Ohta 2011). The first series of experiments were carried out on rock slope models with breakable material under a thrust faulting action with an inclination of 45° (Fig. 15). When layers dip towards valleyside, the ground surface is tilted and the slope surface becomes particularly steeper.

As for layers dipping into mountain side, the slope may become unstable and flexural or columnar toppling failure occurs. Although the experiments are still insufficient to draw conclusions yet, they do show that discontinuity orientation has great effects on the overall stability of slopes in relation to faulting mode. These experiments clearly show that the forced displacement field induced by faulting has an additional destructive effect besides ground shaking on the stability of slopes.

4.3 *Foundations of Bridges*

Several experiments were carried out to investigate the effect of faulting on a bridge and its foundations. The bridge was a truss bridge just over the projected fault line. Fig. 16 shows truss bridge models above the jointed rock mass foundation. Fig. 16(a) shows views of the bridge model before and after the experiments, subjected to the forced displacement field of vertical normal faulting mode. Bridge foundations were pulled apart and tilted. The vertical offset was 0.37 times the bridge span. Similarly, Fig. 16(b) shows the bridge model before and after the experiments subjected to the forced displacement field of 45°

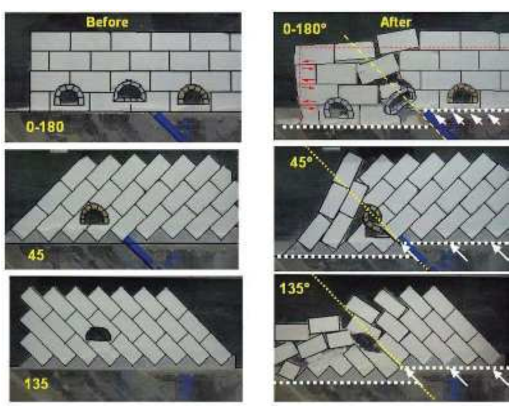

Figure 14. Effect of faulting on underground openings.

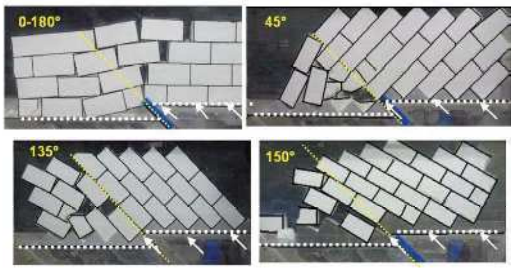

Figure 15. Effect of faulting on rock slopes.

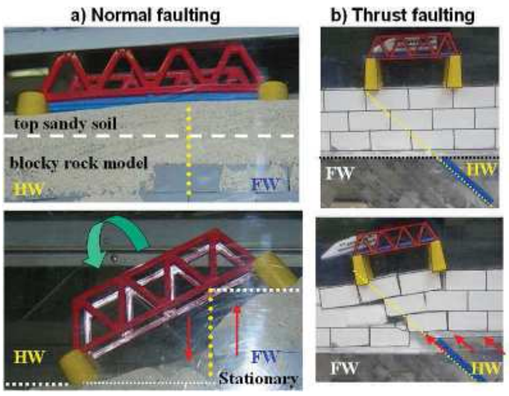

Figure 16. Effect of faulting on foundations of bridges.

thrust faulting mode. Bridge foundations were also pulled apart at the top and compressed at the bottom, and tilted as seen in Fig. 16(b).

4.4 *Embedded Linear Structures (such as Pipelines)*

A series of experiments were carried out on the effect of thrust faulting and normal faulting regarding the embedded linear structures in jointed breakable rock mass model such as pipelines etc. (Figs. 17 and 18). The model rock mass was layered with vertical cross joints. Furthermore, a house model was put on top of the projected tip of the fault. When

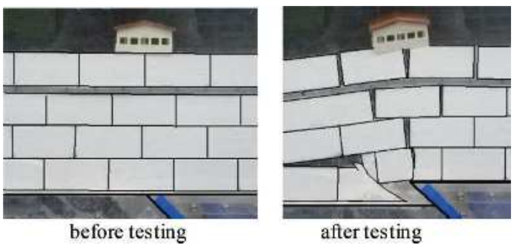

Figure 17. Deformation of embedded linear structure subjected to 45 degree thrust faulting.

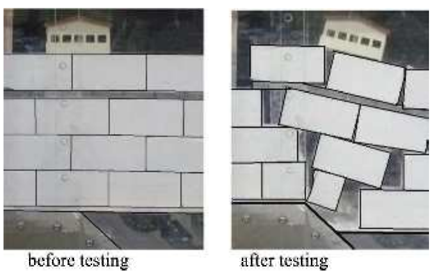

Figure 18. Deformation of embedded linear structure subjected to 45 degree normal faulting.

the thrust faulting is considered, the embedded linear structure deforms to accommodate faulting displacement. In addition, inter-slip among blocks occurs and some are separated and rotated. The block close to the fault tip is fractured. When the normal faulting is considered, the embedded linear structure deforms to accommodate faulting displacement. In addition, inter-slip among blocks and linear embedded structure occurs and some of blocks are separated and rotated. The block close to the fault tip is also fractured.

5 CONCLUSIONS

The following conclusions may be drawn from this experimental study as follow:

1. Dynamic component of faulting is an important factor governing the shape of deformed ground, ground surface structures and slip-lines compared with those observed in faulting experiments using constant velocity type experimental devices.
2. The volume of deformed ground is larger in experiments with dynamic component compared with those from the constant velocity experiments.
3. If the vertical component of faulting is large enough to induce ground failure on the stationary side, the ground surface would be stablised at an inclination equivalent to the dynamic repose angle of non-cohesive material.
4. The damage state may differ depending upon the location of tunnels with respect to fault movement. The damage of tunnels may be quite heavy if they are projection line of motion.
5. The experiments on slopes indicated that discontinuity orientation of rock mass has great effects on the overall stability of slopes in relation to faulting mode. The forced displacement field induced by faulting has an additional destructive effect besides ground shaking on the stability of slopes.
6. Bridge foundations may be pulled apart and tilted. Bridge foundations subjected to the forced displacement field of 45° thrust faulting mode. were also pulled apart at the top and compressed at the bottom, and tilted.
7. The embedded linear structures deform to accommodate faulting displacement and inter-slip among blocks occurs and some are separated and rotated. The block close to the fault tip is fractured.

REFERENCES

Aydan, Ö., 2003. Actual observations and numerical simulations of surface fault ruptures and their effects engineering structures. *The Eight U.S.-Japan Workshop on Earthquake Resistant Design of Lifeline Facilities and Countermeasures Against Liquefaction*. Technical Report, MCEER-03-0003, 227–237.

Aydan Ö, 2012. Ground motions and deformations associated with earthquake faulting and their effects on the safety of engineering structures. Encyclopedia of Sustainability Science and Technology, Springer, R. Meyers (Ed.), 3233–3253.

Aydan Ö., Ulusay, R., Hasgür, Z., and Hamada, M. (1999): The Behavior of structures built on active fault zones in view of actual examples from the 1999 Kocaeli and Chi-Chi earthquakes. ITU International Conference on Kocaeli Earthquake, Istanbul, pp.131–142, 1999.

Aydan, Ö., Y. Ohta, Hamada, M. 2009a. Geotechnical evaluation of slope and ground failures during the 8 October 2005 Muzaffarabad earthquake in Pakistan. Journal Seismology, Vol.13, No.3, pp.399–413.

Aydan, Ö., Y. Ohta, M. Hamada, J. Ito, K. Ohkubo, 2009b. The characteristics of the 2008 Wenchuan Earthquake disaster with a special emphasis on rock slope failures, quake lakes and damage to tunnels. Journal of the School of Marine Science and Technology, Tokai University, Vol.7, No.2,pp.1–23,2009.

Aydan, Ö., Hamada, M., Itoh, J, Ohkubo, K., 2009c. Damage to Civil Engineering Structures with an Emphasis on Rock Slope Failures and Tunnel Damage Induced by the 2008 Wenchuan Earthquake. Journal of Disaster Research, Vol.4, No.2, pp.153–164,2009.

Aydan, Ö., Ohta, Y., Genis, M., Tokashiki, N. and Ohkubo, K. 2010. Response and stability of underground structures in rock mass during earthquakes. Rock Mechanics and Rock Engineering, 43(6), 857–875.

Ohta, Y. (2011): A fundamental research on the effects of strong motions and ground deformations in the neighborhood of earthquakes faults on Civil Engineering structures. Doctorate Thesis, Tokai University, Graduate School of Science and Engineering, 285 pages.

Ohta, Y. and Aydan, Ö. 2010. The dynamic responses of geomaterials during fracturing and slippage. Rock Mechanics and Rock Engineering, Vol.43, No.6, 727–740.